Electrocatalysis

DOI: 10.1002/ange.201311099

NHC-Containing Manganese(I) Electrocatalysts for the Two-Electron Reduction of CO_2**

Jay Agarwal, Travis W. Shaw, Charles J. Stanton III, George F. Majetich, Andrew B. Bocarsly, and Henry F. Schaefer III*

Abstract: *The synthesis and characterization of the first catalytic manganese N-heterocyclic carbene complexes are reported: MnBr(N-methyl-N′-2-pyridylbenzimidazol-2-ylidine)$(CO)_3$ and MnBr(N-methyl-N′-2-pyridylimidazol-2-ylidine)$(CO)_3$. Both new species mediate the reduction of CO_2 to CO following two-electron reduction of the Mn^I center, as observed with preparative scale electrolysis and verified with $^{13}CO_2$. The two-electron reduction of these species occurs at a single potential, rather than in two sequential steps separated by hundreds of millivolts, as is the case for previously reported MnBr(2,2′-bipyridine)$(CO)_3$. Catalytic current enhancement is observed at voltages similar to MnBr(2,2′-bipyridine)$(CO)_3$.*

Low-valent manganese(I) complexes of the form *fac*-[MnBr(N–N)$(CO)_3$], where N–N is bare or modified 2,2′-bipyridine (bpy), have recently been identified as electrocatalysts for the two-electron reduction of CO_2 to CO.[1,2] These catalysts offer improvements over rhenium analogues, which have been employed since the 1980s.[3–5] Namely, the one- and two-electron reduction potential for manganese is shifted anodic, yielding a decreased overpotential for CO_2 conversion, and the synthesis is less-expensive, which is due in part to the abundance of manganese metal. Much improvement is still needed, however, to optimize the rate of conversion and further reduce the overpotential.

Central to achieving those goals is investigating new manganese(I) tricarbonyl-type complexes that also exhibit catalytic activity. Several studies have aimed at optimizing the catalytic process through functionalization of the pyridyl ligand or replacement of the axial halogen. Investigations of the former, however, are often limited to ancillary modifications, such as the addition of alkyl substituents at the 4 and 4′ positions on bpy. Modification of the coordinating atom (that is, replacing nitrogen) has received little attention, although this should have a profound effect on the electronic structure.

Herein we report the replacement of one pyridine ring in bpy with an N-heterocyclic carbene (NHC) moiety to afford a *fac*-[MnBr(N–C)$(CO)_3$]-type catalyst. The advantage of this approach lies in the versatility of NHC ligands, which can be 4, 5, or 6-membered and include substitutions for the nitrogen atoms and for the coordinating carbon atom.[6] One disadvantage, however, is the enhanced σ-donor character compared to pyridine that may result in an increased HOMO–LUMO gap and a cathodic shift of the one- and two-electron reduction potentials. Notwithstanding that effect, we sought to integrate NHC-pyridine ligands into the manganese tricarbonyl framework and evaluate their efficacy for CO_2 reduction.

We chose *N*-methyl-*N*′-2-pyridylbenzimidazolium (**L1**) and *N*-methyl-*N*′-2-pyridylimidazolium (**L2**) as model ligands (Scheme 1) for testing the catalytic activity, and to assess the structure–activity relationship of an extended π system. Previously, these ligands were coordinated to Re^I tricarbonyl compounds in photochemical studies by Vaughan,[7] Li,[8] and Casson.[9] Additionally, Chang and co-workers have reported Ni-centered catalysts with related NHC-pyridine ligands for CO_2 reduction.[10,11] To our knowledge, **L1** and **L2** have not been reported in an analogous manganese complex. In fact, few NHC-containing Mn^I complexes are known, and none, of any oxidation state, have been identified as catalysts.[12,13]

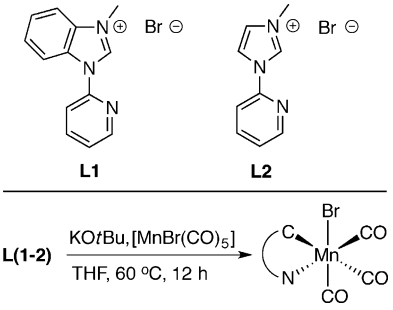

Scheme 1. Ligands under study (top), and chelation strategy (bottom).

Our investigation began with the synthesis of ligands **L1** and **L2** from 2-bromopyridine and benzimidazole or imidazole, respectively.[14] The resulting compounds were *N*-methylated with bromomethane, yielding a Br^- salt. Both **L1**[15] and **L2**[16] were verified with ^{1}H NMR and compared to known

[*] Dr. J. Agarwal, Prof. Dr. H. F. Schaefer III
Center for Computational Quantum Chemistry
University of Georgia (USA)
E-mail: jagarwal@uga.edu
T. W. Shaw, Prof. Dr. A. B. Bocarsly
Department of Chemistry, Princeton University (USA)
C. J. Stanton III, Prof. Dr. G. F. Majetich
Department of Chemistry, University of Georgia (USA)

[**] Research at UGA was supported by the National Science Foundation (NSF), Grant CHE-1054286. Research at Princeton was supported by funding from the DOD-MURI program under AFOSR Award FA9550-10-1-057 and the NSF under grant CHE-1308652. T.W.S. acknowledges the NSF for a graduate research fellowship. We thank Dr. Pingrong Wei for assistance in the acquisition and refinement of X-ray structures, and Dr. Todd Harrop for the use of an infrared spectrometer. NHC = N-heterocyclic carbene.

Supporting information for this article is available on the WWW under http://dx.doi.org/10.1002/anie.201311099.

values.[17] Our choice of the bromo salt stems from its solubility in water, which allows for facile removal upon aqueous workup after chelation. Each ligand was chelated to pentacarbonylbromomanganese [$MnBr(CO)_5$] at 60 °C in THF for 12 h under argon with excess KO*t*Bu. [$MnBr(\mathbf{L1})(CO)_3$] (**1**)[18] and [$MnBr(\mathbf{L2})(CO)_3$] (**2**)[19] were verified by FTIR, ^{1}H NMR, and ^{13}C NMR. Single crystals of **1** suitable for X-ray analysis were grown from slow diffusion of hexanes into a solution of **1** in chloroform (Figure 1). Detailed experimental procedures for all transformations are given in the Supporting Information.

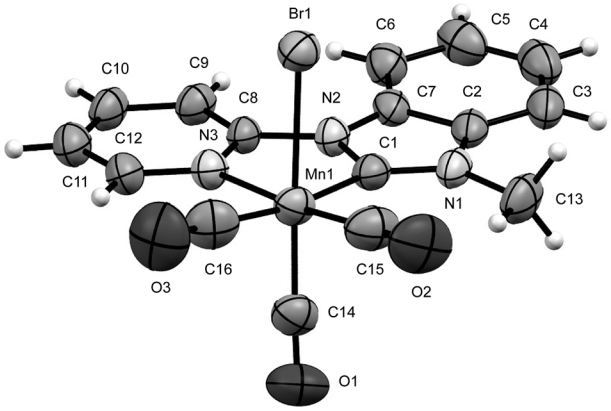

Figure 1. [$MnBr(\mathbf{L1})(CO)_3$] (**1**) from crystal structure; ellipsoids are set at 50% probability.[23] Selected bond lengths [Å]: Mn1–C1 1.984(4), Mn1–C14 1.794(4), Mn1–C15 1.795(4), Mn1–C16 1.828(5), Mn1–N3 2.060(3), N2–C8 1.399(4).

The cyclic voltammetry of **1** under argon in wet (5% H_2O) CH_3CN shows two irreversible redox processes at −1.35 V vs. the saturated calomel electrode (SCE) and −1.64 V vs. SCE, as shown in Figure 2. The peak current of the first reduction wave demonstrates a linear dependence on the square root of the scan rate, indicating a diffusion-limited process (see the Supporting Information). At successively faster scan rates, the second redox process decreases in current until it can no longer be seen at all (500 mV s^{-1} or greater). Therefore, the second reduction wave corresponds to a species formed at the first reduction. No other reductive processes were observed when the cyclic voltammetric window was expanded to the onset of solvent reduction (roughly −3.0 V vs. SCE).

Under an atmosphere of CO_2, the current doubles from 0.18 mA cm^{-2} to 0.36 mA cm^{-2} at the first reduction wave, indicating catalytic turnover. Compared to [$MnBr(bpy)(CO)_3$] under the same conditions, the first reduction wave of **1** occurs at a similar voltage to the second one-electron reduction wave of [$MnBr(bpy)(CO)_3$]. As such, the catalytic current enhancement for each species has a similar onset. As noted previously, the presence of water is necessary for catalytic activity.[1,2] Accordingly, when cyclic voltammetry was performed in dry CH_3CN there was no significant difference in current between argon and CO_2 saturated electrolytes.

The cyclic voltammetry of **2** under argon in wet (5% H_2O) CH_3CN is similar to that of **1**. Two irreversible redox processes occur at −1.46 V vs. SCE and −1.72 V vs. SCE, as shown in Figure 3. These events are shifted cathodically by 110 mV and 80 mV, respectively, from **1**. We attribute this shift to the decreased π*-accepting ability of the coordinating

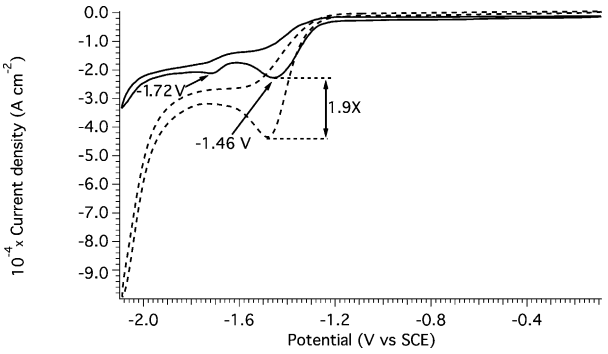

Figure 3. Cyclic voltammagram of [$MnBr(\mathbf{L2})(CO)_3$] (**2**) under Ar (solid) and CO_2 (dashed) in wet (5% H_2O) CH_3CN with 0.1 M tetrabutylammonium perchlorate (TBAP) supporting electrolyte at 10 mV s^{-1}. Complex **1** was loaded at a concentration of 1 mM, and the pH adjusted to 3.7 ($HClO_4$) in the case of Ar.

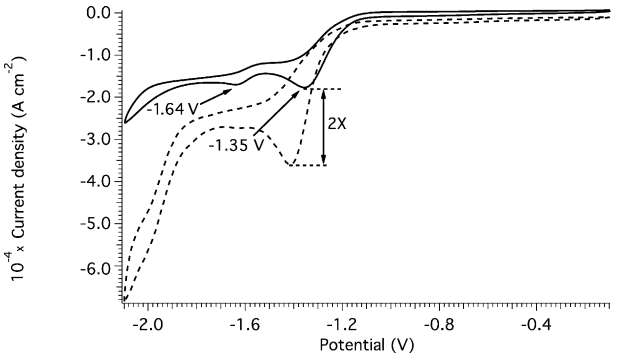

Figure 2. Cyclic voltammagram of [$MnBr(\mathbf{L1})(CO)_3$] (**1**) under Ar (solid) and CO_2 (dashed) in wet (5% H_2O) CH_3CN with 0.1 M tetrabutylammonium perchlorate (TBAP) supporting electrolyte at 10 mV s^{-1}. Complex **1** was loaded at a concentration of 1 mM, and the pH adjusted to 3.7 ($HClO_4$) in the case of Ar.

carbon atom as a result of removing the annulated benzene ring,[20] yielding increased net electron donation to the metal center.[21] Comparing the symmetric CO stretching frequencies[22] for **1**[18] (2015 cm^{-1}) and **2**[19] (2012 cm^{-1}) demonstrates this effect; increased electron density at the metal center results in additional carbonyl π*-backbonding that weakens the C≡O bond and reduces the stretching frequency.

Under an atmosphere of CO_2, **2** shows a current enhancement of 1.9× at the first reduction wave; slightly less than found for **1**, though both fall below the same enhancement in [$MnBr(bpy)(CO)_3$] (2.7×). From previously published equations for the turnover frequency (TOF),[2] we calculated a TOF for **1** and **2** as 0.08 s^{-1} and 0.07 s^{-1}, respectively. For reference, our calculated TOF for [$MnBr(bpy)(CO)_3$] under the exact same conditions is 0.14 s^{-1} (see the Supporting Information). To further confirm the electrocatalytic conversion of CO_2 to CO in the compounds under study, we

electrolyzed **1** at the potential of the first peak in the presence of $^{13}CO_2$. After passing nine coulombs, we evacuated the headspace of the electrolysis cell and examined it with FTIR spectroscopy. The presence of ^{13}CO confirms successful conversion (see the Supporting Information).

From these data, we postulated that **1** and **2** behave similarly to [MnBr(bpy)$(CO)_3$] where a two-electron reduction of the metal center yields a five-coordinate anion that ligates and reduces CO_2. [MnBr(bpy)$(CO)_3$] displays two sequential reductions, however, that occur several hundred millivolts apart; the first reduction likely forms a neutral radical after bromide loss, and the second reduction yields the requisite anion. Only one reduction wave is observed for **1** and **2**, yet they are able to mediate a $2e^-$ process, consistent with an ECE mechanism.

To gather support for this hypothesis, we looked at the reversibility of the redox process as a function of scan rate for complex **2** (Figure 4).At scan rates below 100 mV s^{-1} the process appears nonreversible. Assuming the reaction course is an electrochemical step (reduction of **2**), a chemical step (loss of bromide), and a final electrochemical step (reduction

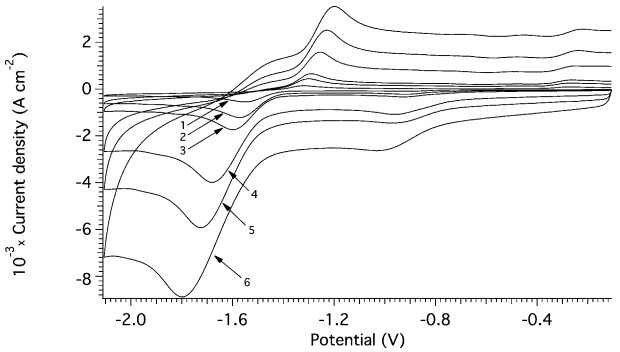

Figure 4. Cyclic voltammetry of **2** (1 mM) at 100 mV s^{-1}, 500 mV s^{-1}, 1 V s^{-1}, 5 V s^{-1}, 10 V s^{-1}, and 20 V s^{-1} (traces 1 to 5, respectively) in dry CH_3CN under argon with 0.1 M tetrabutylammonium perchlorate (TBAP) supporting electrolyte.

of the neutral radical), the nonreversibility at slower scan rates can be attributed to a fast irreversible chemical step following the initial electron transfer. At faster scan rates (greater than 100 mV), the reaction displays quasi-reversible behavior, suggesting that the loss of bromide is slower than reoxidation for the radical anion formed upon initial reduction. This suggests that the species formed at the first reduction wave corresponds to the anionic [Mn(**L2**)$(CO)_3]^-$ species. The second, smaller peak (−1.72 V vs. SCE for **2**) likely corresponds to reduction of a limited quantity of dimer, [{Mn(**L2**)$(CO)_3\}_2$], formed from the first process. This notion is supported by the observed redox potential for the manganese bpy dimer, [{Mn(bpy)$(CO)_3\}_2$], that occurs cathodic to the first electron reduction.

Lastly, as a preliminary test of the selectivity and robustness of the catalysts under study, we conducted three four-hour electrolysis trials of **2** at the potential of the first peak under an atmosphere of CO_2. Every hour we sampled the headspace and examined the concentration of CO and H_2 using gas chromatography (GC). Importantly, we did not observe H_2 production at any point, which illustrates the excellent selectivity for reduction of CO_2 to CO. Steady production of CO was observed throughout the electrolysis, with an average Faradaic efficiency of 34.6 % at the four hour mark. A summary of the electrolysis data is provided in the Supporting Information.

In summary, we have reported the synthesis of two new manganese complexes that contain N-heterocyclic carbene ligands: [MnBr(*N*-methyl-*N*′-2-pyridylbenzimidazol-2-ylidine)$(CO)_3$] and [MnBr(*N*-methyl-*N*′-2-pyridylimidazol-2-ylidine)$(CO)_3$]. Subsequently, we have evaluated their promise for CO_2 reduction and find they are both capable of mediating a two-electron reduction to CO. To our knowledge, this is the first report of catalytic manganese organometallic species that contain NHC ligands. Notably, the first- and second-electron reduction processes for both catalysts occur at approximately the same voltage. Thus, even though the strong σ-donor character of the NHC ligand pushes the reduction potentials cathodic, both species exhibit catalytic current enhancement at voltages comparable to [MnBr(2,2′-bipyridine)$(CO)_3$]. Our hope is that the numerous possibilities for functionalizing NHC ligands will allow for rapid and significant optimization of these promising catalysts.

Received: December 20, 2013
Published online: April 2, 2014

Keywords: carbon dioxide · catalysis · electrochemistry · manganese · N-heterocyclic carbenes

[1] M. Bourrez, F. Molton, S. Chardon-Noblat, A. Deronzier, *Angew. Chem.* **2011**, *123*, 10077 – 10080; *Angew. Chem. Int. Ed.* **2011**, *50*, 9903 – 9906.
[2] J. M. Smieja, M. D. Sampson, K. A. Grice, E. E. Benson, J. D. Froehlich, C. P. Kubiak, *Inorg. Chem.* **2013**, *52*, 2484 – 2491.
[3] J. M. Lehn, R. Ziessel, *Proc. Natl. Acad. Sci. USA* **1982**, *79*, 701 – 704.
[4] B. P. Sullivan, C. M. Bolinger, D. Conrad, W. J. Vining, T. J. Meyer, *J. Chem. Soc. Chem. Commun.* **1985**, 1414 – 1415.
[5] B. Kumar, M. Llorente, J. Froehlich, T. Dang, A. Sathrum, C. P. Kubiak, *Annu. Rev. Phys. Chem.* **2012**, *63*, 541 – 569.
[6] M. Asay, C. Jones, M. Driess, *Chem. Rev.* **2011**, *111*, 354 – 396.
[7] J. G. Vaughan, B. L. Reid, S. Ramachandani, P. J. Wright, S. Muzzioli, B. W. Skelton, P. Raiteri, D. H. Brown, S. Stagni, M. Massimilano, *Dalton Trans.* **2013**, *42*, 14100 – 14114.
[8] X. W. Li, H. Y. Li, G. F. Wang, F. Chen, Y. Z. Li, T. X. Chen, Y. X. Zheng, Z. L. Ling, *Organometallics* **2012**, *31*, 3829 – 3835.
[9] L. A. Casson, S. Muzzioli, P. Raiteri, B. W. Skelton, S. Stagni, M. Massi, D. H. Brown, *Dalton Trans.* **2011**, *40*, 11960 – 11967.
[10] V. S. Thoi, N. Kornienko, C. G. Margarit, P. Yang, C. J. Chang, *J. Am. Chem. Soc.* **2013**, *135*, 14413 – 14424.
[11] V. S. Thoi, C. J. Chang, *Chem. Commun.* **2011**, *47*, 6578 – 6580.
[12] S. Díez-González, N. Marion, S. P. Nolan, *Chem. Rev.* **2009**, *109*, 3612 – 3676.
[13] S. J. Hock, L. A. Schaper, W. A. Herrmann, F. E. Kühn, *Chem. Soc. Rev.* **2013**, *42*, 5073 – 5089.
[14] A. Raba, M. R. Anneser, D. Jantke, M. Cokoja, W. A. Herrmann, F. E. Kühn, *Tetrahedron Lett.* **2013**, *54*, 3384 – 3387.
[15] **L1**: ^{1}H NMR ([D$_6$]DMSO, 20 °C): δ = 10.56 (1 H, s), 8.78 (1 H, d, J = 4 Hz), 8.48–8.46 (1 H, m), 8.31–8.26 (1 H, m), 8.15–8.13 (1 H,

m), 8.06 (1H, d, $J = 8$ Hz), 7.81–7.75 (2H, m), 7.72–7.69 (1H, m), 4.20 ppm (3H, s).

[16] **L2**: ^{1}H NMR ([D$_6$]DMSO, 20 °C): $\delta = 10.08$ (1H, s), 8.64 (1H, d, $J = 8$ Hz), 8.51 (1H, s), 8.23–8.19 (1H, m), 8.03 (1H, d, $J = 8$ Hz), 7.98 (1H, s), 7.65–7.62 (1H, m), 3.97 ppm (3H, s).

[17] G. J. Barbante, P. S. Francis, C. F. Hogan, P. R. Kheradmand, D. J. D. Wilson, P. J. Barnard, *Inorg. Chem.* **2013**, *52*, 7448 – 7459.

[18] **1**: IR ν_{CO} (ATR): 2015 (s), 1927 (m, sh), 1897 cm^{-1} (s). ^{1}H NMR ([D$_6$]DMSO, 20 °C): $\delta = 9.05$ (1H, d, $J = 10$ Hz), 8.53 (1H, d, $J = 10$ Hz), 8.45 (1H, d, $J = 5$ Hz), 8.28–8.25 (1H, m), 7.95 (1H, d, $J = 5$ Hz), 7.62–7.52 (3H, m), 4.33 ppm (3H, s). ^{13}C NMR ([D$_6$]DMSO, 25 °C): $\delta = 225.24$, 221.15, 217.38, 216.30, 154.40, 153.49, 142.00, 137.24, 130.71, 125.29, 125.20, 123.07, 113.72, 112.96, 112.36, 35.32 ppm.

[19] **2**: IR ν_{CO} (ATR): 2012 (s), 1906 cm^{-1} (br). ^{1}H NMR ([D$_6$]DMSO, 20 °C): $\delta = 8.92$ (1H, d, $J = 5$ Hz), 8.46 (1H, s), 8.23–8.21 (1H, m), 8.14 (1H, d, $J = 10$ Hz), 7.72 (1H, s), 7.49–7.46 (1H, m), 4.05 ppm (3H, s). ^{13}C NMR ([D$_6$]DMSO, 25 °C): $\delta = 225.93$, 221.73, 217.64, 201.78, 153.79, 152.96, 141.67, 127.09, 123.33, 117.37, 112.57, 38.06 ppm.

[20] O. Back, M. Henry-Ellinger, C. D. Martin, D. Martin, G. Bertrand, *Angew. Chem.* **2013**, *125*, 3011 – 3015; *Angew. Chem. Int. Ed.* **2013**, *52*, 2939 – 2943.

[21] O. Kühl, *Functionalized N-Heterocyclic Carbene Complexes*, Wiley, Chichester, **2010**.

[22] W. A. Herrmann, J. Schütz, G. D. Frey, E. Herdtweck, *Organometallics* **2006**, *25*, 2437 – 2448.

[23] CCDC 978160 (**1**) contains the supplementary crystallographic data for this paper. These data can be obtained free of charge from The Cambridge Crystallographic Data Centre via www.ccdc.cam.ac.uk/data_request/cif.

